

LOAD MARGIN DETERMINATION METHOD OF INTEGRATED ELECTRICITY-GAS SYSTEM BASED ON CONTINUOUS MULTI-ENERGY FLOW

Bofeng Luo¹, Bo Zhao², Chouwei Ni², Yunfei Mu^{1*}, Xianjun Meng¹, Xiaodan Yu¹, Hongjie Jia¹

1 Key Laboratory of Smart Grid of Ministry of Education (Tianjin University), Tianjin, China

2 State Grid Zhejiang Electric Power Research Institute, Hangzhou, China

ABSTRACT

Load margin is a critical index of voltage security of power systems, which reflects the ability of maintaining system voltage stability when disturbances occur. Nowadays natural gas units (NGUs) are widely used in power system. However the gas supply and the constraints of natural gas systems (NGSs) are not considered in existing load margin determination methods of power systems. In this paper, a load margin determination method for integrated electricity-gas system (IEGS) based on continuation multi-energy flow (CMEF) is proposed. Firstly, a multi-energy flow model with IEGS security constraints is built. Secondly, a load growth parameter is introduced and added to the proposed CMEF. Then, the multi-energy flow solution curve is tracked by a prediction-correction process. Finally, the WSCC 9-bus EPSs combined with 6-node NGSs is employed as a test system to illustrate the impact of NGSs static constraints and natural gas supply on the load margin. Numerical results verify the effectiveness of the CMEF.

Keywords: Load margin; Natural gas system; Continuous power flow; Multi-Energy Flow

NONMENCLATURE

Abbreviations

NGU	natural gas-fired unit
EPS	electrical power system
NGS	natural gas system
IEGS	integrated electricity-gas system
CPF	continuation power flow
CMEF	continuation multi-energy flow

Indices

m, n	indices of nodes in NGS
i, j	indices of bus in EPS

Variables

V_i	voltage magnitude of bus i
ϑ_i	voltage angle of bus i
p_m	gas pressure of node m
f_{mn}	natural-gas flow through pipeline mn
s_{mn}	the flow direction of natural gas
$L_{s,m}$	natural-gas supply at node m
$L_{l,m}$	natural-gas load at node m
P_i^{sp}	active power injection of bus i
Q_i^{sp}	reactive power injection of bus i
G_{ij}	conductance of the bus admittance matrix
B_{ij}	susceptance of the bus admittance matrix
$P_{g,i}$	active power generation of bus i
$P_{l,i}$	active power load of bus i
$Q_{g,i}$	reactive power generation of bus i
$Q_{l,i}$	reactive power load of bus i
$P_{g,i0}$	initial active power generation of bus i
$P_{l,i0}$	initial active power load of bus i
$Q_{l,i0}$	initial reactive power load of bus i
$L_{l,m0}$	initial natural-gas load at node m

Parameters

p_m^{min}	minimum gas pressure at node m
p_m^{max}	maximum gas pressure at node m
V_i^{min}	minimum voltage magnitude at bus i
V_i^{min}	minimum voltage magnitude at bus i
$L_{u,i}$	gas consumption of i th NGU
$P_{u,i}$	active power generation of i th NGU
a_i, b_i, c_i	consumption coefficients of i th NGU
λ	the growth parameter
$K_{g,v}^p, K_{l,v}^p, K_{l,v}^q, K_{l,m}^l$	direction of growth

1. INTRODUCTION

In recent years, the share of natural gas-fired units (NGUs) continues to rise due to its low pollution, short respond time and high efficiency (compared with coal-fired units) [1]. With the linkage become strengthened,

electrical power systems (EPSs) and natural gas system (NGSs) merge to form an integrated electricity-gas system (IEGS) [2]. Therefore, the interaction among NGSs and EPSs are highly concerned [3].

Nowadays, many researches have been carried out on IEGS [4-7]. In [4], the power-to-gas technology is applied to accommodate more renewable energies. In [5], aiming at minimizing the operating cost, a coordinated operation model of IEGS based on linearized coupling relationship is established. In [6], the role of demand response in the optimization of the stochastic day-ahead scheduling with NGSs constraints is studied. However, researches above mainly focus on improving energy efficiency and renewable energy accommodation through multi-energy interaction. More attentions should be paid on the static security analysis of the IEGS [7].

Load margin is an important index of voltage security of power systems, which indicates the distance between current operation point to the security boundary [8]. As a result, it is important to determine the load margin considering the closely linkage between the EPSs and NGSs [9]. The existing load margin determination methods are mainly classified into two types: optimal power flow methods in [10-11] and continuous power flow methods in [12-13]. The former turns the security boundary determination to non-linear optimization, and the result is highly relied on the selected optimization method. For large EPSs, the mostly result of load margin determination are merely locally optimal solution [10]. The continuous power flow method is able to improve the convergence capability of the iterative process, even near the boundary, which is widely used in load margin determination of EPSs [13].

However, the existing load margin determination methods don't take the constraints of NGSs into consideration, and the result is optimistic. For this reason, this paper proposes a load margin determination method for IEGS based on a novel continuous multi-energy flow.

2. MULTI-ENERGY FLOW MODEL WITH IEGS SECURITY CONSTRAINTS

A Multi-energy flow model of IEGS includes a NGS model, an EPS model, and a NGU model.

2.1 Natural gas system model

The variables of NGSs are gas injection and nodal pressure. The nodes in NGSs are divided into two types. One is the injection-known nodes and the other one is the pressure-known nodes. Gas source is set to be the

slack node, whose pressure is known while gas load node pressure is unknown. The gas flow from node m to node n depends on the pressure difference between the two nodes and the pipeline parameters. Then the natural gas flow f_{mn} is given by Eqs. (1)-(2).

$$f_{mn} = c_{mn} s_{mn} \sqrt{s_{mn} (p_m^2 - p_n^2)} \quad (1)$$

$$s_{mn} = \begin{cases} +1 & p_m \geq p_n \\ -1 & p_m < p_n \end{cases} \quad (2)$$

where c_{mn} is the resistance coefficient of the pipeline, which is related to the roughness, diameter and length of this pipeline.

At any node in the NGSs, the inflow and outflow flows must be balanced, as given in Eq. (3).

$$L_{s,m} - L_{l,m} - \sum_{m \in n} f_{mn} = 0 \quad (3)$$

In the NGS, Low gas pressure may lead to abnormal status of insufficient gas supply. When the NGSs approaches to the security boundary, a little change in natural gas demand will lead to one or more violations of IEGS security constraints. Therefore, apart from the natural gas flow equality constraints, the performance of NGSs is also restricted by the inequality constraints. The limitations of nodal pressure are given in Eq. (4).

$$p_m^{\min} \leq p_m \leq p_m^{\max} \quad (4)$$

2.2 Electrical power system model

The power system model is described as Eqs. (5)-(6).

$$P_i^{sp} - V_i \sum_{j \in i} V_j (G_{ij} \cos \vartheta_{ij} + B_{ij} \sin \vartheta_{ij}) = 0 \quad (5)$$

$$Q_i^{sp} - V_i \sum_{j \in i} V_j (G_{ij} \sin \vartheta_{ij} - B_{ij} \cos \vartheta_{ij}) = 0 \quad (6)$$

The power balance of each bus in EPSs should be satisfied in Eqs. (7)-(8).

$$P_i^{sp} = P_{g,i} - P_{l,i} \quad (7)$$

$$Q_i^{sp} = Q_{g,i} - Q_{l,i} \quad (8)$$

When we talk about load margin, we are mainly concerned with the voltage magnitude [12], so the voltage constraint can be expressed as Eq. (9).

$$V_i^{\min} \leq V_i \leq V_i^{\max} \quad (9)$$

2.3 NGU model

All NGUs in IEGS are grouped as a set Ω_{NGU} , which can be expressed as Eq. (10).

$$\Omega_{NGU} = \{G_{u,1}, G_{u,2}, \dots, G_{u,N}\} \quad (10)$$

Where $G_{u,i}$ stands for the i -th NGU; N is the total number of the NGUs.

Then the power injected vector \mathbf{W} of NGUs in the system is expressed as Eq. (11).

$$W = [P_{U,1}, P_{U,2}, \dots, P_{U,N}]^T \quad (11)$$

The NGU generate electricity by consuming natural gas, and the relationship between its natural gas consumption and the electric power output is depicted as Eq. (12).

$$L_{U,j} = a_j + b_j P_{U,j} + c_j P_{U,j}^2 \quad (12)$$

The multi-energy flow model with IEGS security constraints is composed of Eqs. (1)-(9) and Eq. (12).

3. LOAD MARGIN DETERMINATION METHOD BASED ON CONTINUOUS MULTI-ENERGY FLOW

Analogy to Continuation Power Flow (CPF) of EPS, a continuation multi-energy flow (CMEF) is proposed to track the solution curve of multi-energy flow. By adding a continuity parameter to conventional multi-energy flow model, the CMEF overcomes the problem that multi-energy flow model cannot be solved when IEGS is at low-voltage or low-pressure condition.

The parameter λ is used to represent the growth of the generators and load.

$$P_{g,j}(\lambda) = P_{g,j0} + \lambda K_{g,j}^P \quad (13)$$

$$P_{l,j}(\lambda) = P_{l,j0} + \lambda K_{l,j}^P \quad (14)$$

$$Q_{l,j}(\lambda) = Q_{l,j0} + \lambda K_{l,j}^Q \quad (15)$$

$$L_{l,m}(\lambda) = L_{l,m0} + \lambda K_{l,m}^L \quad (16)$$

As shown in figure 1, with the increase of λ , the voltage and pressure will decrease continuously until the security boundary is reached. The CMEF can calculate the voltage and pressure with λ increasing by a prediction and correction process. When tracing the solution curve of multi-energy flow equations, the CMEF will search for the security boundary point by judging whether Eq. (4) or Eq (9) are satisfied.

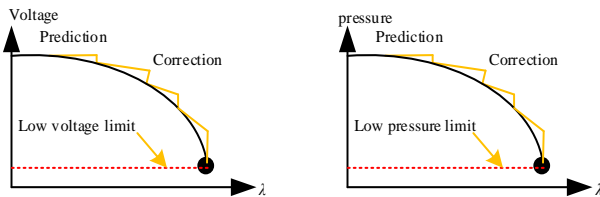


Fig 1 CMEF traces the solution curve of multi-energy flow

When λ are added into the multi-energy flow model, Eqs. (1)-(3), (5)-(8), (10)-(16) are summarized as Eq. (17).

$$H(\mathbf{x}) = 0, \quad \mathbf{x} = (\mathbf{V}, \boldsymbol{\vartheta}, \mathbf{p}, \lambda) \quad (17)$$

Prediction process: if the current solution point is $(\mathbf{V}^{(i)}, \boldsymbol{\vartheta}^{(i)}, \mathbf{p}^{(i)}, \lambda^{(i)})$, computing the tangent vector of the current solution point as the prediction direction for the next solution point, and the tangent vector \mathbf{t} is expressed as Eq. (18).

$$\mathbf{t} = \begin{bmatrix} d\boldsymbol{\vartheta} \\ d\mathbf{V} \\ d\mathbf{p} \\ d\lambda \end{bmatrix} = \begin{bmatrix} \frac{\partial \mathbf{H}}{\partial \boldsymbol{\vartheta}} & \frac{\partial \mathbf{H}}{\partial \mathbf{V}} & \frac{\partial \mathbf{H}}{\partial \mathbf{p}} & \frac{\partial \mathbf{H}}{\partial \lambda} \\ & & \mathbf{e}_k & \end{bmatrix}^{-1} \begin{bmatrix} 0 \\ 1 \end{bmatrix} \quad (18)$$

Calculating the predicted value $(\mathbf{V}^{(i+1)*}, \boldsymbol{\vartheta}^{(i+1)*}, \mathbf{p}^{(i+1)*}, \lambda^{(i+1)*})$ for the next solution point as Eq. (19).

$$\begin{bmatrix} \mathbf{V}^{(i+1)*} \\ \boldsymbol{\vartheta}^{(i+1)*} \\ \mathbf{p}^{(i+1)*} \\ \lambda^{(i+1)*} \end{bmatrix} = \begin{bmatrix} \mathbf{V}^{(i)} \\ \boldsymbol{\vartheta}^{(i)} \\ \mathbf{p}^{(i)} \\ \lambda^{(i)} \end{bmatrix} + \sigma \begin{bmatrix} d\boldsymbol{\vartheta} \\ d\mathbf{V} \\ d\mathbf{p} \\ d\lambda \end{bmatrix} \quad (19)$$

where σ is step length.

Parameterization process: k is a parameter used to determine the position of elements equal to 1 in \mathbf{e}_k . The parameter k selected in prediction process must satisfy Eq. (20).

$$x_k : \max \left\{ \left| \frac{dx_1}{x_1} \right|, \left| \frac{dx_2}{x_2} \right|, \dots, \left| \frac{dx_{n_e-1+n_m+n_g}}{x_{n_e-1+n_m+n_g}} \right| \right\} \quad (20)$$

where n_e , n_m and n_g are the number of EPSs bus, PQ bus and NGSs nodes, respectively.

Correction process: set up CMEF equations according to the parameter k selected in the parameterization process, which is expressed as Eq. (21).

$$\begin{cases} H(\mathbf{x}) = 0 \\ x_k - x_k^* = 0 \end{cases} \quad (21)$$

Taking the predicted value calculated in Eq. (19) as the initial value into the CMEF equations in Eq. (21), the next solution point $(\mathbf{V}^{(i+1)}, \boldsymbol{\vartheta}^{(i+1)}, \mathbf{p}^{(i+1)}, \lambda^{(i+1)})$ is obtained by Newton-Ralph method. Then determine whether the IEGS security constraints in Eq. (4) or Eq (9) are satisfied and go to the prediction process. Until the security constraints are satisfied, the security boundary point is determined.

With the growth of the generators and load as described by Eqs. (13)-(16), the determination of load margin is formulated in Eq. (22).

$$\begin{aligned} & \text{obj max } \lambda \\ & \text{s.t. equality constraint: Eq. (17)} \\ & \text{inequality constraint: Eq. (4), Eq. (9)} \end{aligned} \quad (22)$$

4. CASE STUDY

The proposed approach is verified by a IEGS consisted of a WSCC 9-bus EPS and a modified 6-node NGS through 2 NGUs [14], which is given in Fig. 2. The EB_i and GB_m stand for the buses of EPS and node of NGS, respectively. For WSCC system, EB_1 is the slack bus, EB_2 and EB_3 are PV buses connected with NGU G_2 and G_3 ,

respectively. Parameters of the two NGUs are completely identical.

It is assumed that the voltage range of each bus is 0.75 to 1.05, and the gas pressure range in NGSs is 100 to 450 Psig. The active and reactive power growth directions of every bus in EPSs are the same. The base value of power is 100MW in EPSs. The increase of GB4 and GB6 is the same while the other nodes in NGSs does not increase. The parameters of the growth direction are shown in table I.

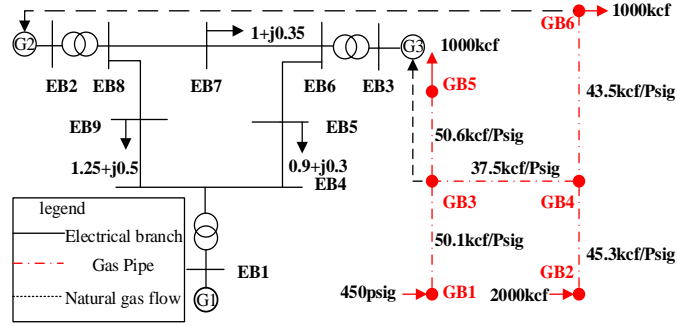


Fig 2 Schematic of the IEGS

TABLE I Direction of growth

$K_{p_o}(p.u.)$	$K_{q_o}(p.u.)$	$K_{v_o}(p.u.)$	$K_{m}(kcf)$
[0.8,0.2]	[0 0.3 0 0.4 0 0.3]	[0 0.3 0 0.4 0 0.3]	[0 0.50 0 50]

In order to highlight the impacts of NGSs security constraint, the load margin in the following scenarios are studied:

Scenario I: Load margin is determined only according to the equality constraints and inequality constraints of EPSs.

Scenario II: Load margin is determined considering equality constraints and inequality constraints of IEGS.

Scenario III: Load margin is determined considering an increase of natural gas load of GB4 to 2000kcf.

The results are shown in Fig. 3 and Fig. 4.

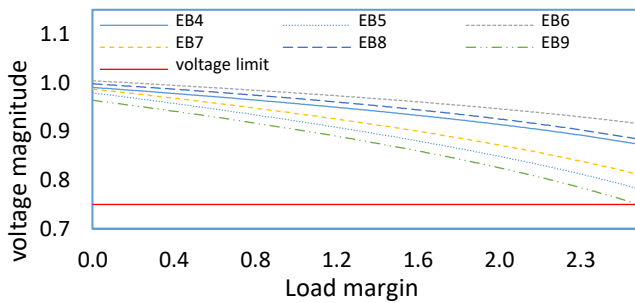
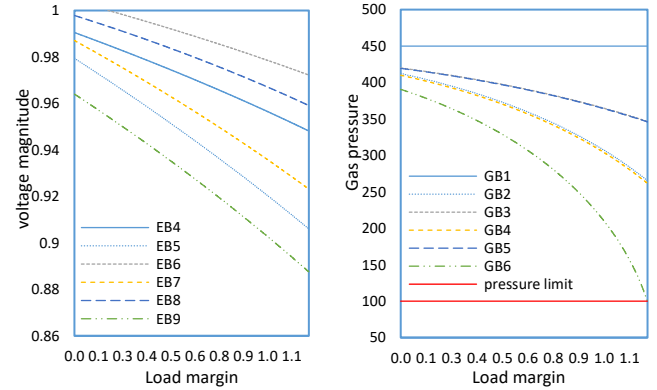


Fig 3 Result of V-λ curve in Scenario I

The results of load margin are shown in table 2, where the state variables of IEGS security boundary point are given, and the key constraints restricting the load margin of IEGS are highlighted in gray background.

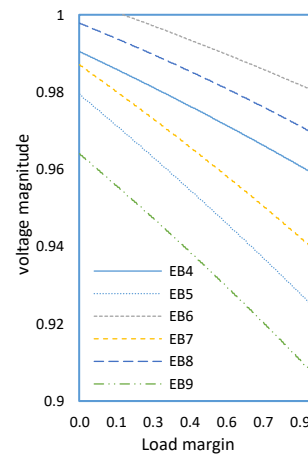
By comparing scenario I and II, the load margin becomes smaller with considering the NGSs constraints. The load margin of scenario I is too optimistic, which may

threaten the security of IEGS. By comparing scenario II and III, the load margin becomes smaller further with the increase of natural gas load. This indicates that if the transmission capacity of NGUs remains unchanged, the increase of natural gas load will squeeze the growth space of load margin.



(a) Result of V-λ curve in Scenario II

(b) Result of p-λ curve in Scenario II



(c) Result of V-λ curve in Scenario III

(d) Result of p-λ curve in Scenario III

Fig 4 CMEF Results in Scenario II and Scenario III

TABLE II Load margin in difference scenario

	Scenario		
	Scenario I	Scenario II	Scenario III
load margin	2.6116	1.2164	0.9244
$v_4(p.u.)$	0.8743	0.9482	0.9595
$v_5(p.u.)$	0.7831	0.9061	0.9255
$v_6(p.u.)$	0.9164	0.9722	0.9808
$v_7(p.u.)$	0.8124	0.9232	0.9403
$v_8(p.u.)$	0.8845	0.9591	0.9699
$v_9(p.u.)$	0.7507	0.8876	0.9081
$p_1(Psig)$	-	450.0000	450.0000
$p_2(Psig)$	-	265.5223	238.8550
$p_3(Psig)$	-	346.6449	339.7253
$p_4(Psig)$	-	261.8260	234.7392
$p_5(Psig)$	-	346.0800	339.1489
$p_6(Psig)$	-	100.3786	101.3989

When the supply of natural gas was increased, such as the natural gas supply of GB2 was increased from 500kcf to 6000kcf, the variations of load margin are shown in figure 5.

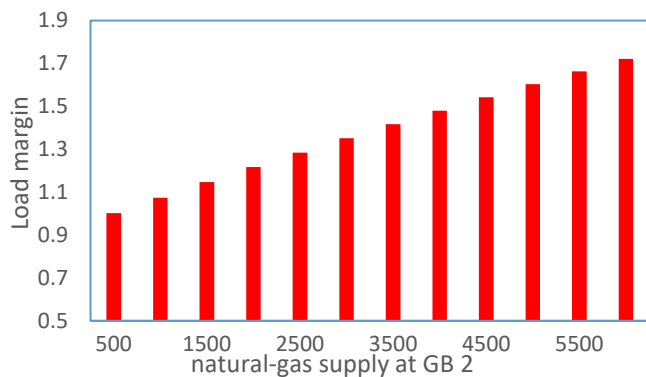


Fig 5 load margin varies with the gas supply

5. CONCLUSIONS

A load margin determination method based on continuous multi-energy flow is proposed, which analyzes the impacts of security constraints of NGSs on load margin. With the rapid rise of electricity generation from NGUs, EPSs is increasingly dependent on the transmission capacity of NGSs. The security constraints have a substantial impact on the value of load margin because the gas fuel of NGUs is not always available. The results of the test case show that:

- 1) CMEF can accurately search the security boundary point and determinate the load margin of IEGS.
- 2) The determination results of the load margin without considering the constraints of NGSs is optimistic in the EPSs with a high ratio of power generation from NGUs.
- 3) The load margin of the power system can be significantly improved by increasing the gas transmission capacity of NGSs.

ACKNOWLEDGEMENT

This work is supported by National Natural Science Foundation of China (No. U1766210) and Research project of State Grid Zhejiang Electric Power Co., Ltd. (5211DS17001D).

REFERENCE

[1]Chen Y, Chua W S, Koch T. Forecasting day-ahead high-resolution natural-gas demand and supply in Germany[J]. Applied energy, 2018, 228: 1091-1110.
 [2]Khan M I, Shahrestani M, Hayat T, et al. Life cycle (well-to-wheel) energy and environmental assessment of natural gas as transportation fuel in Pakistan[J]. Applied Energy, 2019, 242: 1738-1752.

[3]Feijoo F, Iyer G C, Avraam C, et al. The future of natural gas infrastructure development in the United states[J]. Applied Energy, 2018, 228: 149-166.
 [4]Li G, Zhang R, Jiang T, et al. Security-constrained bi-level economic dispatch model for integrated natural gas and electricity systems considering wind power and power-to-gas process[J]. Applied energy, 2017, 194: 696-704.
 [5]Liu J, Wang A, Qu Y, et al. Coordinated operation of multi-integrated energy system based on linear weighted sum and grasshopper optimization algorithm[J]. IEEE Access, 2018, 6: 42186-42195.
 [6]Zhang X, Shahidehpour M, Alabdulwahab A, et al. Hourly electricity demand response in the stochastic day-ahead scheduling of coordinated electricity and natural gas networks[J]. IEEE Transactions on Power Systems, 2016, 31(1): 592-601.
 [7]Qiao Z, Guo Q, Sun H, et al. Static voltage stability margin considering the coupling of natural gas and power system[C]//2018 IEEE Power & Energy Society General Meeting (PESGM). IEEE, 2018: 1-5.
 [8]Xu X, Yan Z, Shahidehpour M, et al. Power system voltage stability evaluation considering renewable energy with correlated variabilities[J]. IEEE Transactions on Power Systems, 2018, 33(3): 3236-3245.
 [9]Fan Y, Liu S, Qin L, et al. A novel online estimation scheme for static voltage stability margin based on relationships exploration in a large data set[J]. IEEE Transactions on Power Systems, 2015, 30(3): 1380-1393.
 [10]Wang C, Cui B, Wang Z, et al. SDP-based Optimal Power Flow with Steady-State Voltage Stability Constraints[J]. IEEE Transactions on Smart Grid, 2018.
 [11]Hashemi S, Aghamohammadi M R, Sangrody H. Restoring desired voltage security margin based on demand response using load-to-source impedance ratio index and PSO[J]. International Journal of Electrical Power & Energy Systems, 2018, 96: 143-151.
 [12]Wang L, Chiang H D. Toward online line switching for increasing load margins to static stability limit[J]. IEEE Transactions on Power Systems, 2016, 31(3): 1744-1751.
 [13]Dong X, Wang C, Yun Z, et al. Calculation of optimal load margin based on improved continuation power flow model[J]. International Journal of Electrical Power & Energy Systems, 2018, 94: 225-233.
 [14]He Y, Yan M, Shahidehpour M, et al. Decentralized Optimization of Multi-Area Electricity-Natural Gas Flows Based on Cone Reformulation[J]. IEEE Transactions on Power Systems, 2017.